

# Optimisation of Multistep Cavity Configuration to Extend Absorption Bandwidth of Micro Perforated Panel Absorber

Iman FALSAFI, Abdolreza OHADI

*Acoustics Research Lab.*

*Department of Mechanical Engineering*

*Amirkabir University of Technology*

No. 424, Hafez Avenue, Tehran 15914, Iran; e-mail: {imann\_fal, a\_r\_ohadi}@aut.ac.ir

(received July 17, 2016; accepted December 21, 2017)

Micro perforated panel (MPP) absorber is a new form of acoustic absorbing material in comparison with porous ones. These absorbers are considered as next generation ones and the best alternative for traditional porous materials like foams. MPP combined with a uniform air gap constructs an absorber which has high absorption but in a narrow bandwidth of frequency. This characteristic makes MPPAs insufficient for practical purposes in comparison with porous materials. In this study instead of using a uniform air gap behind the MPP, the cavity is divided into several partitions with different depth arrangement which have parallel faces. This method improves the absorption bandwidth to reach the looked for goal. To achieve theoretical absorption of this absorber, equivalent electro-acoustic circuit and Maa's theory (MAA, 1998) are employed. Maa suggested formulas to calculate MPP's impedance which show good match with experimental results carried out in previous studies. Electro-acoustic analogy is used to combine MPP's impedance with acoustic impedances of complex partitioned cavity. To verify the theoretical analyses, constructed samples are experimentally tested via impedance tube. To establish the test, a multi-depth setup facing a MPP is inserted into impedance tube and the absorption coefficient is examined in the 63–1600 Hz frequency range. Theoretical results show good agreement compared to measured data, by which a conclusion can be made that partitioning the cavity behind MPP into different depths will improve absorption bandwidth and the electro-acoustic analogy is an appropriate theoretical method for absorption enhancement research, although an optimisation process is needed to achieve best results to prove the capability of this absorber. The optimisation process provides maximum possible absorption in a desired frequency range for a specified cavity configuration by giving the proper cavity depths. In this article numerical optimisation has been done to find cavity depths for a unique MPP.

**Keywords:** micro perforated panel (MPP); multistep cavity; absorption bandwidth; optimisation; impedance tube.

## 1. Introduction

MPPs usually come with an air gap behind them to construct a cavity backed micro perforated panel absorber (CBMPPA). Since the recent decades MP-PAs have been considered a new generation of sound absorbing materials being a substitute for conventional porous materials like foams. MPPs are usually made of metals or plastics (although any rigid materials like glass can be used), so they are fibreless and thus ideal for hygienic conditions indispensable for hospitals, medicine, and food industries (KANG, FUCHS, 1999). Fire proofness, washability, and me-

chanical rigidity give this absorber even more advantage in comparison with porous materials. These properties make them suitable to be used in tough conditions like acoustic shield in engine enclosures (KABRAL *et al.*, 2012), inside mufflers (ALLAM, ÅBOM, 2011; MASSON *et al.*, 2008), or in a wide range of uses like HVAC ducts (LIU *et al.*, 2007) or MRI scanners (LI, MECHEFSKE, 2010).

Absorbing characteristics of MPPAs have been usually investigated for a uniform air gap. This kind of MPPA shows a single absorption peak for each set of geometrical properties, so it can be designed in a way to have a good absorption at a desirable frequency.

Although choosing MPPA's parameters to have a good absorption is possible, the uniform air gap MPPA has a narrow frequency bandwidth due to Helmholtz resonance mechanism. Some studies were done to improve absorption characteristics of MPPAs, especially their absorption bandwidth, like using multilayer MPPs that have uniform air gaps between each of the two layers (RUIZ *et al.*, 2011; ZOU *et al.*, 2006). These MPPAs have a wide bandwidth but occupy large space. The other way is not using a uniform air gap; for example, in Wang's (WANG *et al.*, 2010) study, trapezoidal CBMPPA has been investigated. In another study of Wang (WANG, HUANG, 2011) and Yairi (YAIRI *et al.*, 2011) acoustic properties of MPPA with different cavity depths were investigated.

This article is the following study of conference article (FALSAFI, OHADI, 2015) presented by the same authors. The objective of the article is to achieve a wide uniform bandwidth of absorption (by performing optimisation process); to introduce MPP with multi depth cavity as a practical sound absorbing means, which haven't been considered in previous studies. Another point is focusing on cavities' depth as a key parameter to adjust bandwidth which leads to less expensive sound absorbing material. In this study a multi depth cavity with partitioned sections is studied to investigate bandwidth increasing effect. To do so, two shapes of this configuration (2-steps and 4-steps cavity) with parallel faces are built and tested in the impedance tube to measure absorption characteristics. Maa's theory (MAA, 1998) is used to attain MPP's impedance, and the equivalent electro-acoustic circuit is used to calculate the total impedance of this absorber. By choosing the right equivalent circuit for the MPP combined with these partitioned multistep cavities and using electro-acoustic analogy, equivalent acoustic impedance of absorber can be assessed.

After validation of theoretical results with experimental ones, it's necessary to carry out an optimisation procedure to find the best cavity configuration for a given MPP. The optimisation goal is to maximise absorption in a desired frequency band. Significant engineering results are reachable only after these analyses.

## 2. Theory

### 2.1. Equivalent electric-acoustic circuit analysis

Acoustic characteristics of perforated panels based on propagation of sound waves in narrow tubes first were developed by RAYLEIGH (1896). Then CRANDALL (1926) gave a simplified version for very short tubes in comparison with wavelengths. By considering end corrections, MAA (1975; 1998) developed an approximate formula to calculate micro perforated plate impedance in any range of wave number. Maa's formula shows a good match with experimental results for a MPP

backed by a uniform air gap. MPP impedance can be achieved by Eq. (1), where  $\bar{Z}_{\text{resist}}$  and  $\bar{Z}_{\text{react}}$  are the specific acoustic resistance and reactance of MPP, respectively, which according to Maa's theory can be approximated by Eqs. (2)

$$\bar{Z}_{\text{MPP}} = \bar{Z}_{\text{resist}} + \bar{Z}_{\text{react}}. \quad (1)$$

Impedance with an overline mark indicates specific acoustic impedance which is defined as impedance divided by air impedance ( $\rho_0 c$ )

$$\bar{Z}_{\text{resist}} = \frac{32\mu t}{\rho_0 c \sigma d^2} \left[ \left( 1 + \frac{K^2}{32} \right)^{1/2} + \frac{\sqrt{2}}{32} K \frac{d}{t} \right], \quad (2)$$

$$\bar{Z}_{\text{react}} = j \frac{\omega t}{c \sigma} \left[ 1 + \left( 1 + \frac{K^2}{2} \right)^{-1/2} + 0.85 \frac{d}{t} \right],$$

where  $K = d\sqrt{\rho_0 \omega / 4\mu}$  is the wave number,  $\rho_0$  and  $\mu$  represent density and viscosity of air, respectively,  $c$  denotes the sound velocity in air,  $f$  is the wave frequency as  $\omega = 2\pi f$ , and MPP's characteristics  $t$ ,  $d$ , and  $\sigma$  are MPP's thickness, hole diameter, and perforation ratio, respectively (see Fig. 1). Since the holes are arranged in the square pattern, perforation ratio equals  $\sigma = \pi d^2 / 4b^2$ , where  $b$  represents the distance between two holes.

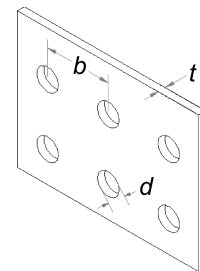


Fig. 1. Schematic representation of MPP parameters.

For a MPP mounted at a distance  $D$  from a rigid wall, the acoustic impedance of air in the cavity can be achieved by Eq. (3)

$$\bar{Z}_{\text{cavity}} = -j \cot \left( \frac{\omega D}{c} \right). \quad (3)$$

In this study a partitioned cavity with stepped configuration has been used. The schematic shape of cavity configurations with different depths have been shown in Fig. 2. Equivalent electro-acoustic circuit is used to calculate absorption coefficient of this cavity configuration and the MPP. In Fig. 3 an equivalent electro-acoustic circuit for a 4-steps cavity configuration is sketched. Any  $n$ -steps cavity configuration's circuit can be constructed likewise. In this circuit, impedance of  $i$ -th branch can be achieved by Eq. (4), where  $\bar{Z}_{D_i}$  is the  $i$ -th cavity impedance from Eq. (3)

$$\bar{Z}_i = \bar{Z}_{\text{MPP}} + \bar{Z}_{D_i}. \quad (4)$$

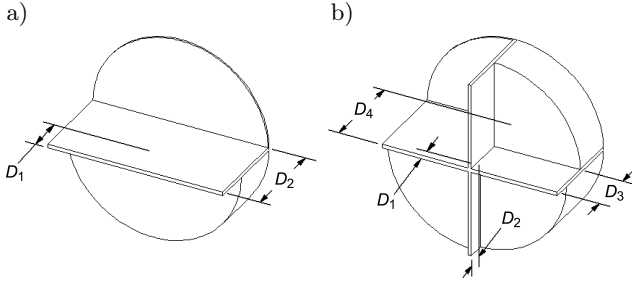


Fig. 2. Cavity configurations: a) 2-steps cavity, b) 4-steps cavity.

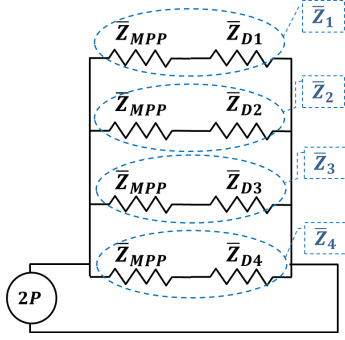


Fig. 3. Equivalent electro-acoustic circuit for a 4-steps cavity configuration.

In these configurations the cavity has been divided into several partitions. If the absorber has the total facing area of  $A$ , each of these uniform air gap partitions covers portion of  $A$  which for the  $i$ -th one corresponding area is  $A_i$ . According to the electrical circuit analysis (YAIRI *et al.*, 2011), the final total impedance of multistep cavity absorber can be computed by Eq. (5). If partitions have equal area surface like the setup arranged for this article, simple Eq. (6) can be used instead of Eq. (5) for a  $n$ -steps cavity configuration. After that, the absorption coefficient can be computed by Eq. (7) at any frequency

$$\frac{1}{\bar{Z}_{\text{total}}} = \frac{1}{A} \sum_{i=1}^n A_i \frac{1}{\bar{Z}_i}, \quad A = \sum_{i=1}^n A_i, \quad (5)$$

$$\frac{1}{\bar{Z}_{\text{total}}} = \frac{1}{n} \sum_{i=1}^n \frac{1}{\bar{Z}_i}, \quad (6)$$

$$\alpha = 1 - \left( \frac{\bar{Z}_{\text{total}} - 1}{\bar{Z}_{\text{total}} + 1} \right)^2. \quad (7)$$

## 2.2. Optimisation

The point of using multistep cavity configuration is to achieve the best cavity depths for each configuration to have most absorption for certain MPP properties. This means the maximum possible bandwidth while

trying to also keep the absorption coefficient maximum. To accomplish this goal, optimisation analysis needs to be done in accordance with the theoretical equations delivered in Subsec. 2.1. In this study numerical optimisation is done to reach optimisation goals. The numerical method is taken in a way that desired cost function has been obtained for any sets of optimisation parameters within the specified allowable ranges of parameters. To achieve various goals, cost functions with different constrains have been applied in two separate procedures, as below. In all analysis MPP's characteristics like thickness ( $t$ ), hole diameter ( $d$ ), and perforation ratio ( $\sigma$ ) are kept fixed and the optimisation process is done on cavity depths ( $D_i$ ) (as optimisation parameters).

### 2.2.1. Procedure 1

In this optimisation procedure the only cost function is maximising the area under absorption curve of each cavity configuration in a desired frequency range. It is just a bound constrained optimisation due to applying the frequency bound. For each set of cavity depths, numerical integration is done in order to calculate the area under the absorption curve.

### 2.2.2. Procedure 2

Here beside of maximising the area under the absorption curve as the cost function, the procedure is restricted to one constraint. The minimum value of the absorption coefficient between each two adjacent peaks of the absorption curve should be greater than a desired absorption value ( $\alpha_{\text{des}}$ ). These falling points of the absorption curve are found by using theoretical formulas and solving the corresponding equations analytically. To do so, after differentiating the absorption relation with respect to frequency and setting  $\alpha/d\omega = 0$ , the obtained equation is solved to find the extremums. Finally, the desired absorption ( $\alpha_{\text{des}}$ ) can be applied to the minimums.

### 2.2.3. Approximations and linearization

According to complex equations for impedances and absorption coefficient, some approximations are taken to theoretically find minimum points of the absorption curve between adjacent peaks. Here, linearisation is done for MPP equations and an approximation is applied for cavity impedances. First, impedance of air in a cavity can be approximated by its Taylor expansion. For that, Eq. (8) is used instead of Eq. (3)

$$\bar{Z}_{\text{cavity}} \cong -j \left[ \frac{1}{\left(\frac{\omega D}{c}\right)} - \frac{\left(\frac{\omega D}{c}\right)}{3} \right]. \quad (8)$$

In addition, since the MPP has constant geometrical properties, its resistance and reactance impedances are simplified with linear equations using the data fitting method.

In this analysis the MPP is a 2.8 mm thick plate ( $t$ ) with 0.6 mm diameter holes ( $d$ ) which are arranged in a square pattern with 4 mm distance between side by side holes ( $b$ ). This MPP is used in experimental tests, as explained in Sec. 1. By fitting a line, resistance and reactance of this MPP can be achieved from relations of Eq. (9), which show a very good matching according to  $R$ -square values (see Fig. 4)

$$\begin{aligned}\bar{Z}_{\text{resist}} &\cong 0.00027104(2\pi\omega) + 0.67341, \\ R^2 &= 0.9995, \\ \bar{Z}_{\text{react}} &\cong j[0.0037809(2\pi\omega) + 0.22143], \\ R^2 &= 0.9933.\end{aligned}\quad (9)$$

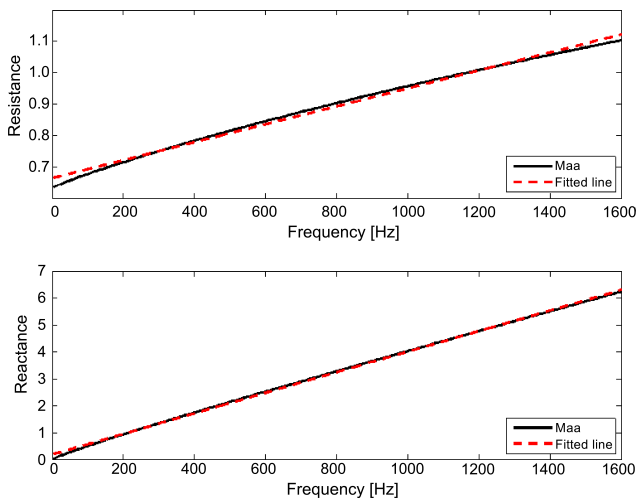


Fig. 4. Resistance and reactance of MPP achieved by Maa's formulas in comparison with the fit lines.

### 2.3. Sensitivity analysis of air gap depth on absorption curve

The main purpose of using multistep cavity configuration and optimising corresponding depths is to achieve the desired goals and improving the absorbing performance of MPP. So, awareness from the effect of cavity depth on absorption behaviour is an important step before doing any further analysis or experimental activities. In this section, sensitivity analysis of uniform air gap ( $D$ ) on absorption of MPP is investigated for a specified MPP. The result can be generalised to obtain sensitivity analysis of MPP with multistep cavities. This sensitivity analysis is done with a 2.8 mm thick MPP with 0.6 mm diameter holes distanced 4 mm in a square pattern (same MPP in Subsec. 2.2.3) and cavity depth changing from 5 to 60 mm. Figure 5 shows the absorption curve for this MPP with different air gap depths.

It can be seen from Fig. 5 that changing air gap's depth has no effect on the value of maximum absorption substantially, whereas it changes the posi-

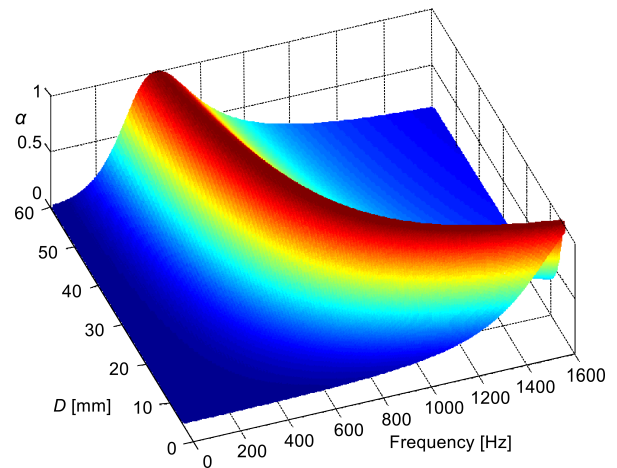


Fig. 5. 3D absorption curve of MPP ( $d = 0.6$ ,  $b = 4$ ,  $t = 2.8$  mm) with various values of air gap depth.

tion of maximum absorption. Absorption peak's shifting has been better presented via absorption contour plot (Fig. 6). This figure indicates that absorption coefficient is more sensitive at lower values of cavity depth. Indeed, for the specified variation of the cavity depth, the change of the frequency of maximum absorption for lower values of cavity depth are much more significant than the corresponding values for higher values of cavity depth.

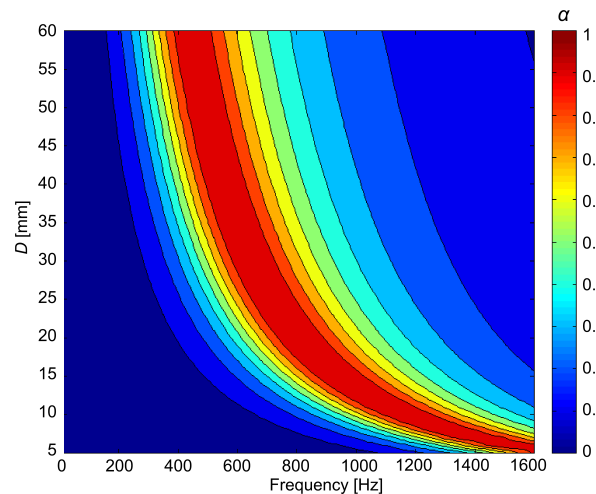


Fig. 6. Absorption contour plot of MPP ( $d = 0.6$ ,  $b = 4$ ,  $t = 2.8$  mm) with various values of air gap depth.

## 3. Experimental test setup

For all experimental tests, a MPP with the geometrical dimensions presented in Table 1 is used, which is

Table 1. Dimensions of MPP used at experimental tests.

	$d$	$b$	$t$
Dimension [mm]	0.60	4.00	2.80

the same as the one that has been mentioned in Subsec. 2.2.3. Each test setup consists of its own cavity backed configuration with a specified MPP.

Each configuration is inserted into impedance tube and the absorption coefficient is examined in the 63–1600 Hz frequency range. Two tested cavity configurations in the impedance tube similar to schematic backings in Fig. 2 are presented in Fig. 7.

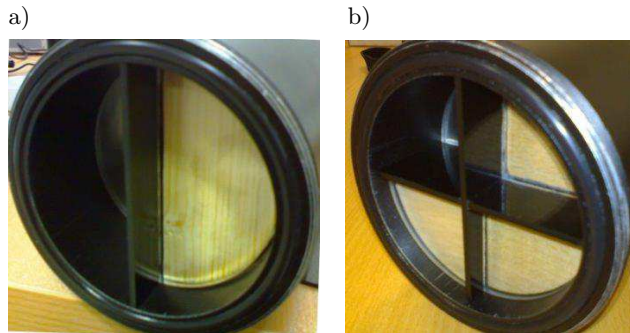


Fig. 7. Cavity configurations in the impedance tube: a) 2-steps cavity, b) 4-steps cavity.

The sound absorption coefficients are measured in accordance with ISO 10534-2 (ISO, 1998) using a 100 mm diameter impedance tube. The impedance tube is the BSWA, SW477+SW422 model of BSWA Technology company. The MPP sample and the impedance tube setup used at the Acoustics Research Laboratory of Amirkabir University of Technology are shown in Fig. 8.

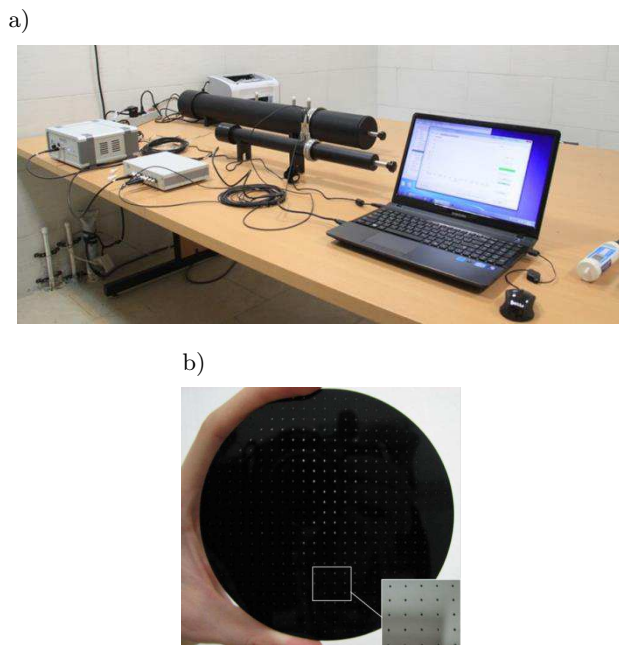


Fig. 8. Experimental test setup: a) impedance tube setup (BSWA, SW477+SW422) at the Acoustics Research Laboratory of Amirkabir University of Technology, b) MPP sample.

## 4. Theoretical and experimental results

### 4.1. Experimental test results

Here the experimental results measured using impedance tube, have been compared with the corresponding theoretical results computed by equivalent electrical circuit introduced in Sec. 2. Initially, results of arbitrary cavity configurations that have been constructed and tested by FALSAFI and OHADI (2015) are represented here. The cavity depths of two configurations are as in Table 2.

Table 2. Cavity depths of two configurations (see Fig. 2).

Configuration type	Depth [mm]			
	$D_1$	$D_2$	$D_3$	$D_4$
2-steps cavity	50	21	–	–
4-steps cavity	45.2	25.6	10.2	7

Here the results of 4-steps cavity configuration are presented based on (FALSAFI, OHADI, 2015). Equation (10) was used to calculate total impedance of the 4-steps cavity configuration theoretically and the result is represented in Fig. 9

$$\frac{1}{\bar{Z}_{\text{total}}} = \frac{1}{4} \left[ \frac{1}{\bar{Z}_{\text{MPP}} + \bar{Z}_{D_1}} + \frac{1}{\bar{Z}_{\text{MPP}} + \bar{Z}_{D_2}} + \frac{1}{\bar{Z}_{\text{MPP}} + \bar{Z}_{D_3}} + \frac{1}{\bar{Z}_{\text{MPP}} + \bar{Z}_{D_4}} \right]. \quad (10)$$

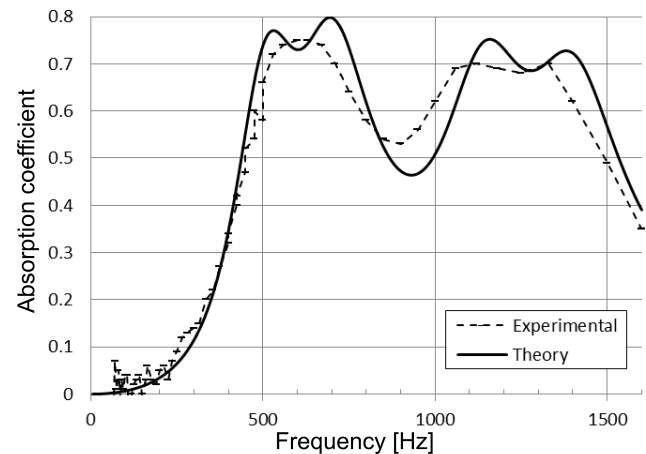


Fig. 9. Experimental and theoretical results of absorption coefficient for the 4-steps cavity configuration ( $D_1 = 45.2$ ,  $D_2 = 25.6$ ,  $D_3 = 10.2$ ,  $D_4 = 7$  mm) (FALSAFI, OHADI, 2015).

The results show a very good agreement between experimental and theoretical results, which indicates that the theory based on equivalent electrical circuit determines the absorption coefficient with the acceptable accuracy. The slight difference may be a consequence of measuring accuracy. For example in Fig. 9, there is

a small frequency difference between the experimental and theoretical results, especially for the two peaks above 1000 Hz. This is especially due to the measured values of the cavity depth. As described in Subsec. 2.3, the absorption coefficient is sensitive to this parameter, especially for lower values of the cavity depth. Also, the absorption curve of each configuration matches its shape. This means that for the  $n$ -steps cavity configuration,  $n$  peaks can be seen respectively; although if resonances of the cavities are close, it would result in only one peak with a larger amplitude.

#### 4.2. Optimisation results

With good agreement between the theoretical and experimental results, some optimisation analyses can be done using theoretical and numerical procedures. The analysis goal is to achieve the best cavity depths for each configuration to have best absorption for certain MPP properties. This means the maximum possible bandwidth while trying to keep the absorption as high as possible.

Here, two procedures mentioned in Subsec. 2.2.1 and 2.2.2 are carried out in two frequency ranges. The purpose of using two ranges of frequency is observing frequency bound effect on the results. Each of these optimisations is done for the 2-steps and 4-steps cavity configurations for the considered cavity depth limits that are listed in Table 3. All of these optimisations are done numerically according to Subsec. 2.2 with 1 mm precision. It means optimisation parameters ( $D_i$ ) have been found with 1 mm accuracy. This precision is adequate and more important, practical in constructing experimental setups. In Table 3, the upper limit is due to space occupation and the lower limit is set so as to

keep the absorption peaks below 1600 Hz. It can be mentioned that 1600 Hz is the upper measuring limit of impedance tube (large tube).

It should be known that no absorption at certain frequency was considered desirable in these analyses. The optimisation analysis results with corresponding conditions are reported in Table 4.

It can be seen that considering the minimum desired absorption constraint ( $\alpha_{des} = 0.8$ ) in 400–1000 Hz frequency range does not affect the results (compare setups number 1 and 2 for 2-step cavity configuration and setups number 5 and 6 for 4-step cavity configuration in Table 4). For this reason, only setups 2 and 5 have been experimentally tested. Figures 11 to 15 indicate the variation of absorption coefficient versus

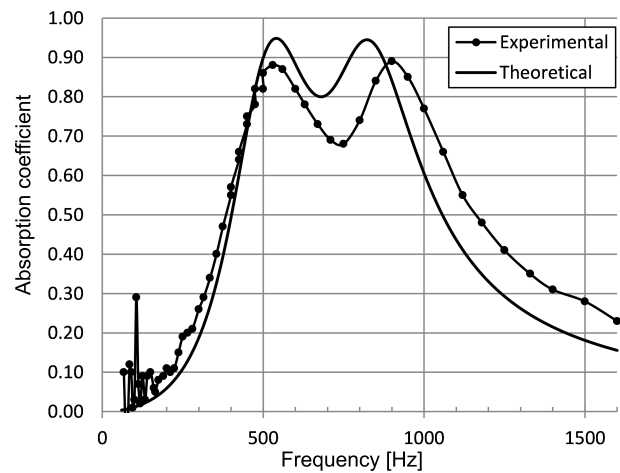


Fig. 10. Setup 2: Optimised 2-steps cavity configuration for frequency range of 400–1000 Hz and not considered  $\alpha_{des}$  ( $D_1 = 19$  and  $D_2 = 46$  mm).

Table 3. Cavity depth limits in optimisation process.

Configuration type	Depth lower limit [mm]	Depth upper limit [mm]
2-steps cavity	7	55
4-steps cavity	7	55

Table 4. Optimised cavity depths for each cavity configuration and optimisation conditions.

Configuration type	Setup number	Optimisation frequency range [Hz]	Constraint: minimum desired absorption ( $\alpha_{des}$ )	Depth [mm]			
				$D_1$	$D_2$	$D_3$	$D_4$
2-steps cavity	1	400–1000	0.8	20	46	–	–
	2	400–1000	Not considered	19	46	–	–
	3	400–1600	0.7	12	27	–	–
	4	400–1600	Not considered	9	31	–	–
4-steps cavity	5	400–1000	0.8	15	23	37	55
	6	400–1000	Not considered	15	21	36	55
	7	400–1600	0.7	9	12	21	36
	8	400–1600	Not considered	7	11	21	45

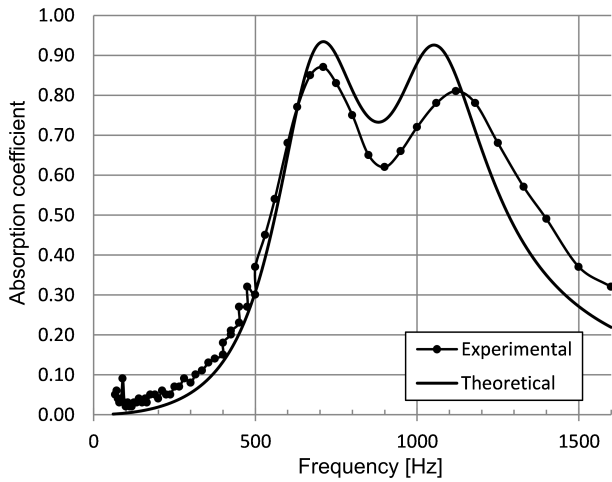


Fig. 11. Setup 3: Optimised 2-steps cavity configuration for frequency range of 400–1600 Hz and  $\alpha_{des} = 0.7$  ( $D_1 = 12$  and  $D_2 = 27$  mm).

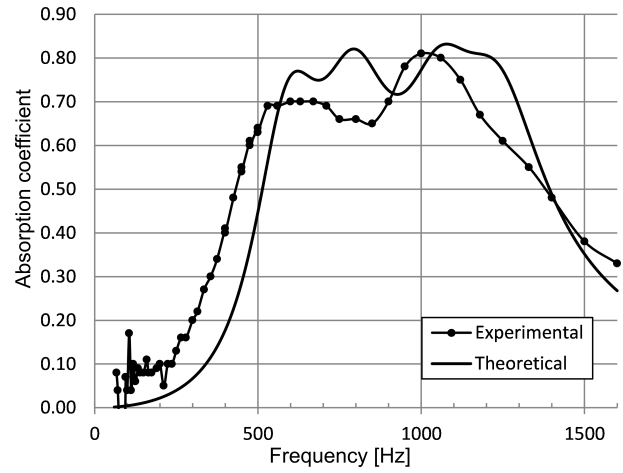


Fig. 14. Setup 7: Optimised 4-steps cavity configuration for frequency range of 400–1600 Hz and  $\alpha_{des} = 0.7$  ( $D_1 = 9$ ,  $D_2 = 12$ ,  $D_3 = 21$  and  $D_4 = 36$  mm).

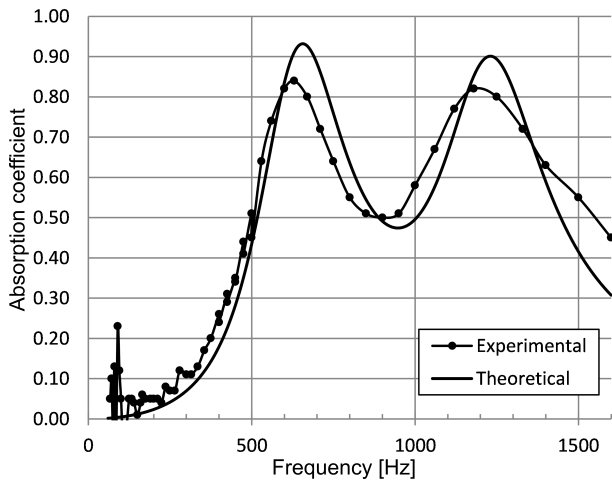


Fig. 12. Setup 4: Optimised 2-steps cavity configuration for frequency range of 400–1600 Hz and not considered  $\alpha_{des}$  ( $D_1 = 9$  and  $D_2 = 31$  mm).

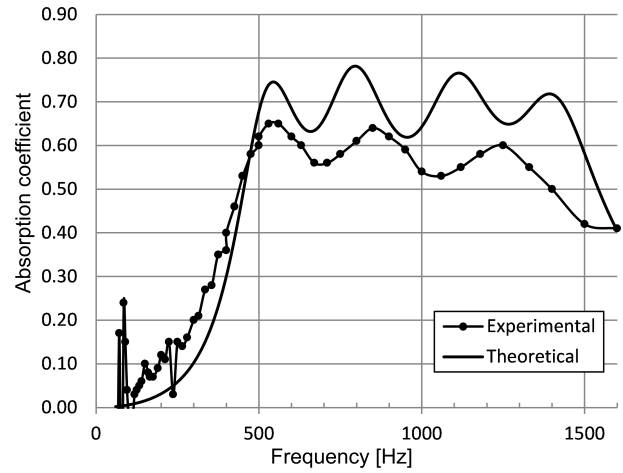


Fig. 15. Setup 8: Optimised 4-steps cavity configuration for frequency range of 400–1600 Hz and not considered  $\alpha_{des}$  ( $D_1 = 7$ ,  $D_2 = 11$ ,  $D_3 = 21$  and  $D_4 = 45$  mm).

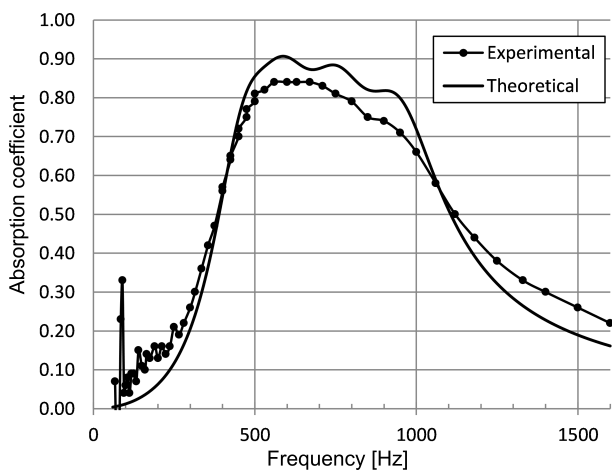


Fig. 13. Setup 5: Optimised 4-steps cavity configuration for frequency range of 400–1000 Hz and  $\alpha_{des} = 0.8$  ( $D_1 = 15$ ,  $D_2 = 23$ ,  $D_3 = 37$  and  $D_4 = 55$  mm).

frequency for optimised 2 and 4 steps configurations. Acceptable agreement between theoretical and experimental results can be seen in all figures. The difference at some setups, especially at higher frequencies, is due to an inaccuracy of building cavity configuration, as the sensitivity of the acoustical performance of the system to cavity depth has been discussed at Subsec. 2.3.

The optimised results indicate the necessity of obtaining the optimised values of cavity depths. Without optimisation process, this shape of absorber would not result in good and wide band absorption. Usage of optimised cavity depth guarantees maximum possible bandwidth beside of achieving good absorption. This can be seen especially for the 4-steps cavity configuration which has a good smooth uniform curve in a wide range of frequency. In order to see optimisation effect, comparisons between optimised and non-

optimised results are presented in Figs. 16 and 17 for two and four steps cavity configurations, respectively. According to Fig. 16, there is a wide band of absorption for 2-steps cavity type MPPA after optimisation. In this figure, the frequency range of optimisation procedure is 400–1600 Hz (as shown in Fig. 12). In addition, Fig. 17 indicates that besides the wide band of absorption, optimised 4-steps configuration has much smoother behaviour, as expected.

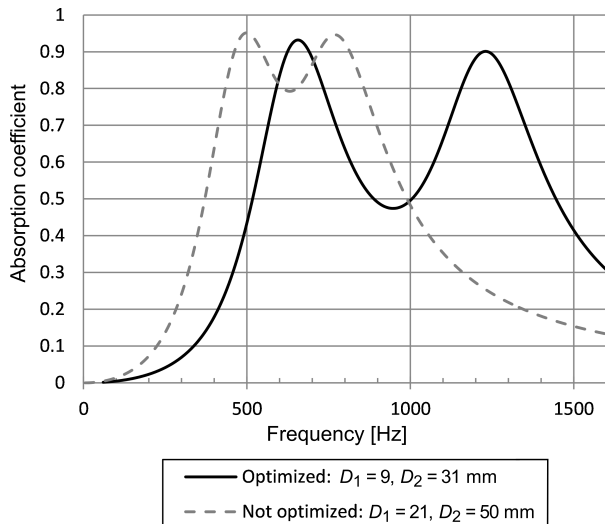


Fig. 16. Comparison of optimised and not-optimised 2-steps cavity backing MPPA.

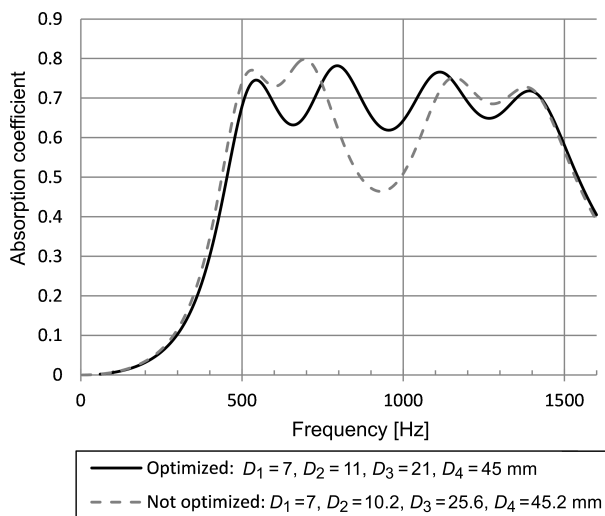


Fig. 17. Comparison of optimised and not-optimised 4-steps cavity backing MPPA.

The obtained results point out that applying the desired absorption to keep the minimums above the desired value does not affect the results for analyses in the 400–1000 Hz frequency range. On the other hand, in a wider frequency range like 400–1600 Hz, this constraint has a considerable influence on acoustical performance of the system.

Also by comparing the results, one can see that there is a trade-off between achieving wide band-

width and high absorption. Indeed, for the wider frequency bandwidth, the absorption peaks are decreased. As a matter of fact increasing the number of cavities causes widening of the bandwidth although the maximum absorption peaks are reduced, as expected. Again, it should be emphasised that changing the cavity depth would shift MPP's absorption peak, but practically doesn't affect its absorption coefficient (go to Subsec. 2.3). To understand the physical reason, by considering the 2-steps cavity configuration, two peaks can be seen. The reason is that half of sound wave goes through each cavity and for each cavity depth there is one absorption peak at a certain frequency. So the absorption capability of the system is divided into two frequency ranges. The result is that absorption for the total absorber would be lower than the peak for one partition cavity configuration.

## 5. Conclusion

In this study the cavity behind the MPP has been partitioned into several separate sections with different depths. By means of this method, widening the frequency bandwidth of absorption has been investigated. This multi depth cavity helps the absorber to have a wider bandwidth rather than a uniform air gap MPPA. Although, for a certain number of partitions in cavity configuration, there is a balance between the wide band and smooth high absorption. The simulation results using the equivalent electro-acoustic circuit based on Maa's theory matches the corresponding experimental results, so the theoretical conclusions have been approved.

Afterward an optimisation process has been carried out to find the best cavity configuration so as to achieve maximum bandwidth and absorption coefficient. This optimisation results in a wide absorption bandwidth at the best possible absorption. But it is not possible to reach a higher level uniform absorption in a wide range of frequency. Another conclusion from optimisation results is that by increasing the number of partitions in the cavity, a wide uniform range of absorption can be attained but maximum absorption would be dropped.

At the end it can be concluded that this method, choosing MPP's parameters and working on cavities' depth to adjust bandwidth, is a simple, inexpensive, and adequate way of improving absorption characteristics of MPP absorbers, which makes them to have practical engineering and architectural acoustics usage, and also candidate them as a suitable substitution for fibrous materials.

## References

1. ALLAM S., ÅBOM M. (2011), *A new type of muffler based on microperforated tubes*, Journal of vibration

- and acoustics, **133**, 3, 031005, doi: 10.1115/1.4002956.
2. CRANDALL I.B. (1926), *Theory of vibrating systems and sound*, D. Van Nostrand Company, New York.
  3. FALSAFI I., OHADI A. (2015), *Improving absorption bandwidth of micro-perforated panel by stepping the cavity*, [in:] Proceedings of 22nd International Congress on Sound and Vibration, Vol. 2, M.J. Crocker, F. Pedrielli, S. Luzzi, M. Pawelczyk, E. Carletti [Eds.], pp. 3828–3835, Florence, Italy, 12–16 July.
  4. ISO 10534-2 (1998), *Acoustics-determination of sound absorption coefficient and impedance in impedance tubes – Part 2: Transfer-function method*.
  5. KABRAL R., RÄMMAL H., LAVRENTJEV J. (2012), *Acoustic Studies of Micro-Perforates for Small Engine Silencers*, SAE Technical Paper 2012-32-0107, <https://doi.org/10.4271/2012-32-0107>.
  6. KANG J., FUCHS H. (1999), *Predicting the absorption of open weave textiles and micro-perforated membranes backed by an air space*, Journal of Sound and Vibration, **220**, 5, 905–920, doi: 10.1006/jsvi.1998.1977.
  7. LI G., MECHEFSKE C.K. (2010), *A comprehensive experimental study of micro-perforated panel acoustic absorbers in MRI scanners*, Magnetic Resonance Materials in Physics, Biology and Medicine, **23**, 3, 177–185, doi: 10.1007/s10334-010-0216-9.
  8. LIU J., HERRIN D., SEYBERT A. (2007), *Application of micro-perforated panels to attenuate noise in a duct*, SAE Technical Paper 2007-01-2196, <https://doi.org/10.4271/2007-01-2196>.
  9. MAA D.Y. (1975), *Theory and design of microperforated panel sound-absorbing constructions*, Scientia Sinica, **18**, 1, 55–71.
  10. MAA D.Y. (1998), *Potential of microperforated panel absorber*, Journal of the Acoustical Society of America, **104**, 5, 2861–2866, doi: 10.1121/1.423870.
  11. MASSON F., KOGAN P., HERRERA G. (2008), *Optimization of muffler transmission loss by using microperforated panels*, FIA2008, Buenos Aires.
  12. RAYLEIGH J.W.S.B. (1896), *The theory of sound*, Vol. 2, Macmillan, London.
  13. RUIZ H., COBO P., JACOBSEN F. (2011), *Optimization of multiple-layer microperforated panels by simulated annealing*, Applied Acoustics, **72**, 10, 772–776, doi: 10.1016/j.apacoust.2011.04.010.
  14. WANG C., CHENG L., PAN J., YU G. (2010), *Sound absorption of a micro-perforated panel backed by an irregular-shaped cavity*, Journal of the Acoustical Society of America, **127**, 1, 238–246, doi: 10.1121/1.3257590.
  15. WANG C., HUANG L. (2011), *On the acoustic properties of parallel arrangement of multiple microperforated panel absorbers with different cavity depths*, Journal of the Acoustical Society of America, **130**, 1, 208–218, doi: 10.1121/1.3596459.
  16. YAIRI M., SAKAGAMI K., TAKEBAYASHI K., MORIMOTO M. (2011), *Excess sound absorption at normal incidence by two microperforated panel absorbers with different impedance*, Acoustical Science and Technology, **32**, 5, 194–200, doi: 10.1250/ast.32.194.
  17. ZOU J., SHEN Y., YANG J., QIU X. (2006), *A note on the prediction method of reverberation absorption coefficient of double layer micro-perforated membrane*, Applied Acoustics, **67**, 2, 106–111, doi: 10.1016/j.apacoust.2005.05.004.